This is the preprint version of our accepted manuscript published on 22 July 2022 in Langmuir : https://pubs.acs.org/doi/10.1021/acs.langmuir.2c01122

Bifunctional Calix[4]arene-coated Gold Nanoparticles for Orthogonal Conjugation

Maurice Retout,[a] Benedetta Cornelio,[b] Gilles Bruylants*,[a] and Ivan Jabin*,[b]

[a] *Université libre de Bruxelles (ULB), Engineering of Molecular Nanosystems, 50 Avenue F.D. Roosevelt, 1050 Bruxelles, Belgium*

[b] *Université libre de Bruxelles (ULB), Laboratoire de Chimie Organique, CP 160/06, 50 Avenue F.D. Roosevelt, 1050 Bruxelles, Belgium*

gilles.bruylants@ulb.be; Ivan.Jabin@ulb.be

Keywords: Calixarenes • Diazoniums • Nanoparticles • Conjugation • Mixed Layers • Bifunctional MNPs

Graphical Abstract

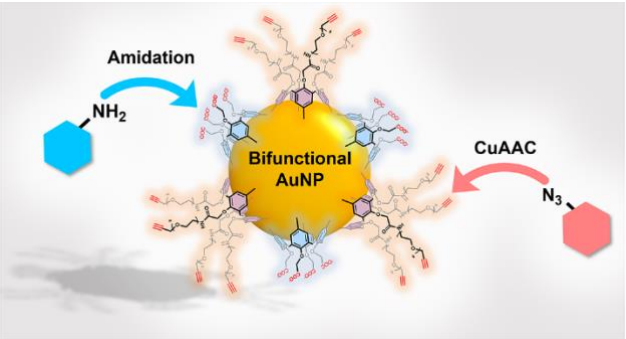

Abstract

Gold nanoparticles (AuNPs) are currently intensively exploited in the biomedical field as they possess interesting chemical and optical properties. Although their synthesis is well-known, their controlled surface modification with defined densities of ligands such as peptides, DNA, or antibodies remains challenging and has generally to be optimized case by case. This is particularly true for applications like *in vivo* drug delivery that require AuNPs with multiple ligands, for example a targeting ligand and a drug in well-defined proportions. In this context, we aimed to develop a calixarene-modification strategy that would allow the controlled orthogonal conjugation of AuNPs respectively via amide bond formation and copper(I)-catalyzed azide-alkyne cycloaddition (CuAAC). To do this, we synthesized a calix[4]arene-tetradiazonium salt bearing four PEG chains ended by an alkyne group (**C1**) and, after optimization of its grafting on 20 nm AuNPs, we demonstrated that CuAAC can be used to conjugate an azide containing dye (N_3-cya7.5). It was observed that AuNPs coated with **C1** (AuNPs-**C1**) can be conjugated to approximately 600 N_3-cya7.5 that is much higher than the value obtained for AuNPs decorated with traditional thiolated PEG ligands terminated by an alkyne group. The control over the number of molecules conjugated via CuAAC was even possible by incorporating a non-functional calixarene (**C2**) in the coating layer. We then combined **C1** with a calix[4]arene-tetradiazonium salt bearing four carboxyl groups (**C3**) that allows conjugation of an amine (NH_2-cya7.5) containing dye. The conjugation potential of these bifunctional AuNPs-**C1**/**C3** was quantified by UV-Vis spectroscopy: AuNPs decorated with equal amount of **C1** and **C3** could be conjugated to approximately 350 NH_2-dyes and 300 N_3-dyes using successively amide bond formation and CuAAC, demonstrating the control over the orthogonal conjugation. Such nanoconstructs could benefit to anyone in the need of a controlled modification of AuNPs with two different molecules via two different chemistries.

Introduction

During the last decades, nanomedicine has known huge developments in various applications including drug delivery, sensing and imaging.[1–4] Among the different classes of nanomaterials used in this field, gold nanoparticles (AuNPs) are particularly attractive thanks to their ease of synthesis, plasmonic properties,[5,6] biocompatibility and low toxicity,[7] and surface reactivity that allows the anchoring of (bio)molecules.[8–12] In this regard, AuNPs have been notably exploited for the design of *in vitro* sensors,[13,14] as nanocarriers for *in vivo* drug delivery systems,[15,16] or phototherapy hotspots.[17,18] For all these applications, the surface of the AuNPs has to be functionalized in order to increase their stability in complex media or to confer them properties such as biocompatibility or targeting of specific cells/tissues. A possible functionalization strategy consists in grafting a dense layer of organic ligands that further allows the covalent immobilization of (bio)molecules through classical (bio)conjugation reactions (post-functionalization step). Typically, citrate-capped AuNPs are first synthesized and the citrate anions present at the surface are then exchanged with thiol ligands displaying a terminal reactive group.[19] An usual method to prepare AuNPs carrying mixed layers of ligands random spread over the surface with a control over the grafting density, consists in the concomitant addition of two different thiol ligands at specific ratios ("simultaneous" method). Due to the lability of the Au-S bond, it was however shown that the resulting ratio of ligands at the surface may greatly differ from that initially introduced in solution.[20,21] Another classical method for the formation of mixed layers relies on the stepwise addition of different ligands but, in this case, control over the ligands ratio is complicated to obtain and this "stepwise" method has been shown to be more adapted to the formation of Janus-like nanoparticles.[22] The limitations of these two methods is particularly problematic for applications requiring multi-functional AuNPs, for example, when both a targeting ligand and a drug have to be anchored on a same particle.[23–27]

It is known that, upon reduction of their diazonium groups,[28–30] calix[4]arene-tetradiazonium salts[31,32] can form multiple C-metal bonds[33] with the surface of gold or silver nanoparticles, leading to thin and extremely robust organic layers.[34–36] When the calix[4]arene is substituted with a reactive functional group at its small rim (e.g. carboxyl), it is possible to further post-functionalize the nanoparticles with various (bio)molecules.[37,38] Moreover, the irreversible nature of the grafting and the similar reactivity toward surfaces of calix[4]arene-tetradiazonium salts[31,32] bearing different substituents at the small rim allow the formation of mixed layers with control over the proportions of the different calix[4]arenes used.[39,40] We thus envisioned that the calixarene-based methodology could be used for the preparation of AuNPs bearing multiple ligands that would enable further orthogonal (bio)conjugation. For this, the concomitant grafting of calixarenes bearing alkyne or carboxyl groups was envisaged. Indeed, while carboxyl groups can be used for the formation of an amide bond with amine-containing molecules via classical amidation reactions, alkynes can react with azide-containing molecules through the well-known copper(I)-catalyzed azide-alkyne cycloaddition (CuAAC). To our knowledge, bifunctional gold nanoparticles that could be orthogonally post-functionalized by CuAAC and amidation have never been reported in the literature.[41]

Herein, we report on the preparation of AuNPs coated by two different calixarenes with a control over the composition of the mixed layers and the use of these nanoparticles for the orthogonal conjugation of molecules.

Results and Discussion

Preparation of the calix[4]arene-tetradiazonium salts and of the AuNPs. Three calix[4]arene-tetradiazonium salts differing by their substituents at the small rim were used (**Figure 1**). **C1** and **C3** were chosen as their terminal functional groups could be exploited for the further conjugation of (bio)molecules through CuAAC and amidation reactions,

respectively. **C2** bears four PEG chains ended by a methoxy group and was used for optimization and control experiments. Note that **C1** was synthesized in a few steps from commercial *pt*Bu-calix[4]arene-tetraacetic acid tetraethyl ester (see the Experimental section and the SI) while **C2** and **C3** were readily obtained according to literature procedures.[39,42] Water dispersible AuNPs-citrate with a core diameter of 19.7 ± 2.5 nm were synthesized via a modified Turkevich method and used for all the experiments reported in this study. UV-Vis, IR and TEM characterizations are available in Supporting Information (Figures S1 and S2).

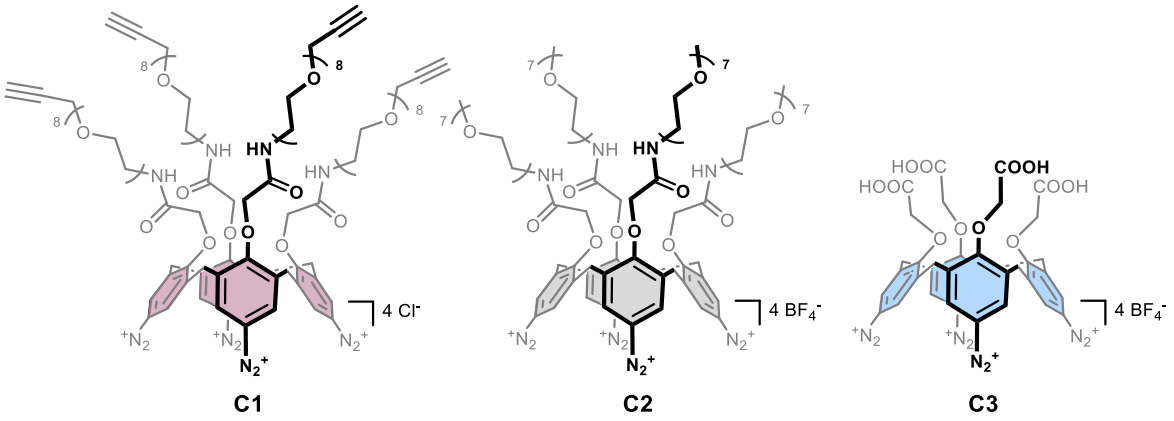

Figure 1. Structure of calix[4]arene-tetradiazonium salts **C1**, **C2** and **C3**.

Preparation, characterization, and post-functionalization of AuNPs bearing alkyne groups. The modification of AuNPs-citrate with the newly synthesized **C1** was first investigated as the grafting of a calix[4]arene-tetradiazonium salt bearing alkyne groups had never been described before. The coating was achieved under reducing conditions through a classical ligand exchange process (**Scheme 1**).[39] Briefly, 2×10^5 **C1**/NP (AuNPs ~10 nM ; **C1**~ 2 mM) were added dropwise and under vigorous stirring to a dispersion of AuNPs-citrate in presence of sodium borohydride (0.5 equiv. per **C1**). After 16 hours of reaction, the resulting water dispersible AuNPs-**C1** were purified from the excess of free calixarenes by centrifugation and replacement of the supernatant by pure water.

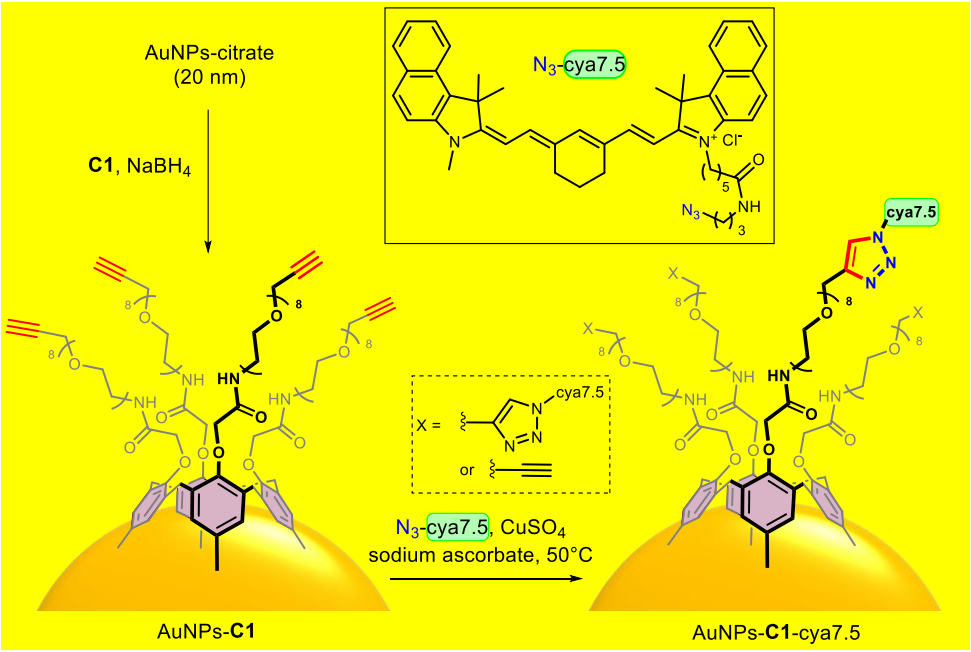

Scheme 1. Synthesis of AuNPs-**C1** and AuNPs-**C1**-cya7.5. Inset: structure of N_3-cya7.5.

Barely no loss of particles was observed by UV−Vis spectroscopy after the functionalization and purification processes but a significant shift of the maximum of absorbance of the LSPR band was observed ($\Delta_{\lambda max}$ > 10 nm) (**Figure 2A**), in agreement with the modification of the AuNPs surface with **C1**. The grafting of **C1** was further confirmed by ATR-FTIR analysis of the particles (**Figure 2B**). In comparison to AuNPs-citrate, asymmetric C-O-C stretching of PEG chains at 1100 cm^{-1}, C_{ar}-C_{ar} ring stretching at 1456 cm^{-1} and amide bands I and II at 1664 and 1542 cm^{-1}, respectively, could be observed on the IR spectrum of AuNPs-**C1**. Furthermore, the signal corresponding to the carboxylate groups of the adsorbed citrates at 1600 cm^{-1} decreased drastically, confirming the success of the ligand exchange process. Unfortunately, signals of the alkyne groups were not intense enough to be observed in the FTIR spectrum, probably because they are too far from the AuNPs surface to benefit from the surface-enhanced infrared absorption effect. It is worth noting that the AuNPs-**C1** expressed high colloidal and chemical stabilities due to the calixarene-based coating. They endured extreme pH (pH1 for 3 hours) or high fluoride concentrations (250 mM for 3 hours) without showing any signs of degradation or aggregation (Figure S3).

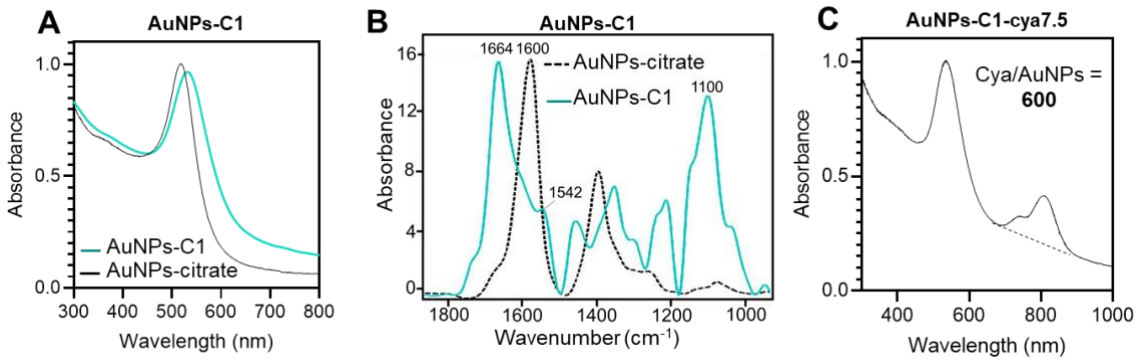

Figure 2. (A) UV-Vis spectra of the AuNPs-citrate (black line) and the AuNPs-**C1** (blue line). **(B)** ATR-FTIR spectra of the AuNPs-citrate (dashed black line) and the AuNPs-**C1** (blue line). **(C)** UV-Vis spectrum of AuNPs-**C1**-cya7.5.

For comparison purpose, AuNPs functionalized with a pegylated thiol derivative bearing a terminal alkyne group, i.e. HS-$CH_2CH_2(CH_2CH_2O)_{12}$-$CH_2C{\equiv}CH$ (HS-PEG-alkyne), were also prepared under a classical ligand exchange process (see the Experimental section). UV-Vis and FTIR spectra of the resulting nanoparticles (i.e. AuNPs-S-PEG-alkyne) showed respectively a shift of the λ_{max} and the characteristic C-O-C stretching band of the PEG chains, confirming the chemisorption of the thiol derivative on the particles (Figure S4A and S4B).

The conjugation capacity of both AuNPs-**C1** and AuNPs-S-PEG-alkyne was then evaluated through the coupling of a near-infrared cyanine7.5-based dye containing and azido group (i.e. N_3-cya7.5, see **Scheme 1** for the structure of the dye). This dye was chosen as it does not absorb light in the same UV-Vis region than the gold particles (i.e. 805 nm vs 520 nm, respectively), which allows its easy quantification on the AuNP surface by UV-Vis analysis of the AuNPs. The conjugation of N_3-cya7.5 to the particles was achieved in presence of copper sulfate and sodium ascorbate at pH 9 and at 50°C (see **Scheme 1** for AuNPs-**C1**-cya7.5). The conjugated AuNPs-**C1**-cya7.5 and AuNPs-S-PEG-cya7.5 were then cleaned from the excess of reagents and dyes by four cycles of centrifugation, removal of the supernatant and replacement of this latter by an aqueous SDS solution. Densities of approximately 600 ±

55 and 75 ± 15 dyes covalently conjugated per particle were measured by UV-Vis spectroscopy for AuNPs-**C1**-cya7.5 and AuNPs-S-PEG-cya7.5, respectively (Figures **2C** and S4C). Considering the reported grafting density of 0.7/nm² (or 600 per NP of that size) for similar calixarenes,[39] i.e. bearing PEG chains of similar size at the level of their small rim, the dye density measured represents approximately one dye per **C1**. Furthermore, the number of dyes that were covalently conjugated to the AuNPs-**C1** is more than 10 times higher than the one obtained with nanoparticles functionalized by the traditional chemisorption of thiols. Terminal alkyne groups are known to display an affinity for gold surfaces[43,44] and are sometimes exploited to anchor ligands on AuNPs.[45] As a result, only few examples of AuNPs with terminal alkyne groups have been reported in the literature.[46] Thus, the poor ability of AuNPs-S-PEG-alkyne for conjugation through CuAAC may well result from the fact that a large part of the ligands have their terminal alkyne group bound to the surface. In the case of AuNPs-**C1**, the high reactivity of the radicals generated through the reduction of the diazonium groups and the irreversible nature of the calixarene attachment to the surface may explain that most of the calixarene-based ligands are attached through the aryl moieties and that a large number of alkyne groups remains available for coupling.

Having shown that **C1** could be used for the efficient conjugation of azides on AuNPs, we then evaluated the possibility to form mixed layers to control the amount of terminal alkyne groups at the surface of the particles. For this, the grafting of mixtures of calix[4]arene-tetradiazonium salts **C1** and **C2** (with different ratios of **C1/C2**: 100/0, 75/25, 50/50, 25/75 and 0/100) was investigated under similar conditions than detailed previously. In all cases, the total amount of calixarenes was kept constant (i.e. 2×10^5/NP). The resulting various batches of water dispersible AuNPs-**C1/C2** were then analyzed by UV-Vis spectroscopy. A sharp LSPR band was obtained, whatever the composition of the mixed layer (Figure S6). Interestingly, all the AuNPs-**C1/C2** expressed high colloidal and chemical stabilities. As an example, **Figures 3A**

and **3B** show the UV-Vis spectra of AuNPs-**C1/C2** prepared with 50% of **C1** at pH7 and after 3 hours at pH 1 or in 250 mM KF, respectively, showing no degradation of the particles. UV-Vis spectra of AuNPs-**C2** at pH 1 or in 250 mM KF can be found in the Supporting Information, Figure S6. ATR-FTIR analysis of the particles AuNPs-**C1/C2** indicated that, in all cases, a similar amount of calixarenes was grafted onto the AuNPs. However, due to a high similarity between the FTIR spectra of AuNPs-**C1** and AuNPs-**C2**, it was not possible to draw conclusion on the composition of the mixed layer from these analyses (Figure S7). The conjugation of N_3-cya7.5 to the different batches of particles AuNPs-**C1/C2** was achieved under similar conditions than for AuNPs-**C1**. After the usual cleaning process, the dispersions were analyzed by UV-Vis spectroscopy. Very interestingly, a linear relationship was observed between the number of dyes covalently conjugated to the particles and the proportion of **C1** in the grafting solution (**Figure 3C**). This result clearly shows that the ratio of **C1** and **C2** grafted at the AuNPs surface, and thus the amount of conjugated dye, can be controlled by the composition of the grafting solution.

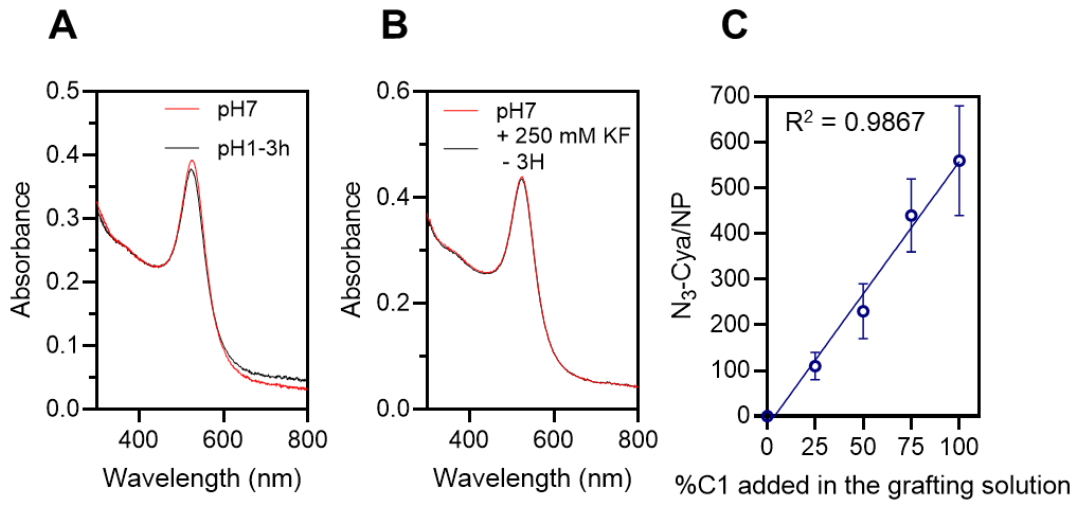

Figure 3. (A) UV-Vis spectra of AuNPs-**C1**/**C2** (50% of **C1**) at pH7 and after suspension at pH1 for 3 hours. **(B)** UV-Vis spectra of AuNPs-**C1**/**C2** (50% of **C1**) at pH7 and after suspension in 250 mM of KF for 3 hours. **(C)** Number of dyes covalently conjugated per particle to the AuNPs-**C1**/**C2**-cya7.5 as a function of the percentage of **C1** used for the functionalization of the particles.

Bifunctional nanoparticles. The production of water dispersible bifunctional AuNPs (i.e. carrying both carboxyl and alkyne groups) was investigated by modifying AuNPs-citrate with a 1:1 mixture of calix[4]arene-tetradiazonium salts **C1** and **C3** (**Scheme 2**). The grafting procedure was similar to what was described previously (10^5 calixarenes/NP). After appropriate cleaning, the resulting AuNPs-**C1/C3** were characterized and compared to AuNPs-**C1** and AuNPs-**C3**.

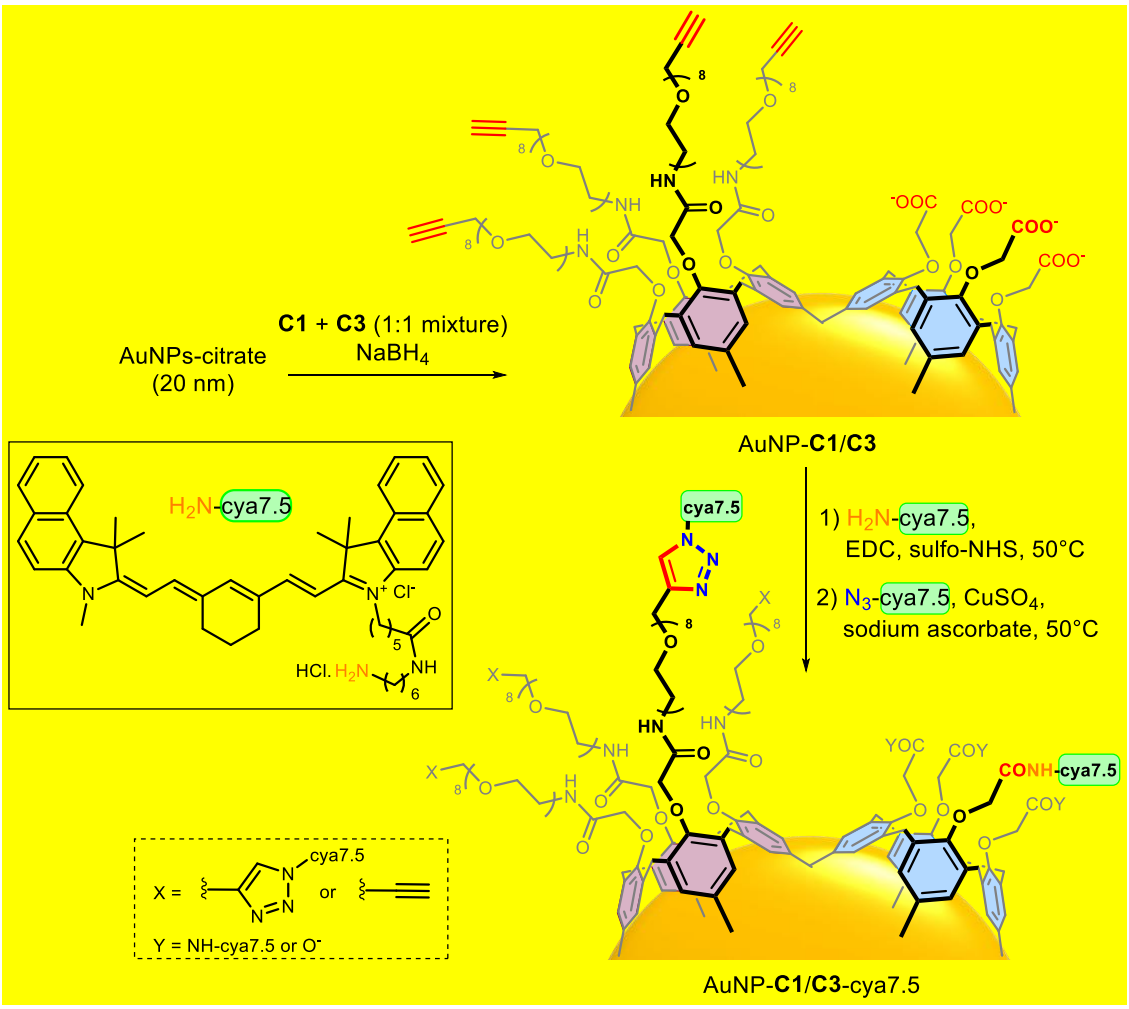

Scheme 2. Synthesis of AuNPs-**C1**/**C3** and AuNPs-**C1**/**C3**-cya7.5. Inset: structure of H_2N-cya7.5.

UV-Vis analysis showed a similar sharp and intense LSPR band for AuNPs-**C1/C3**, AuNPs-**C1** and AuNPs-**C3** (**Figures 4A-C**). It is worth noting that AuNPs-**C1/C3** expressed a similar stability toward KF addition than AuNPs-**C1** or AuNPs-**C2** (Figure S8). More

interesting, when the spectra were recorded at pH7 then 2 (addition of HCl) and finally back to 7 (further addition of NaOH), a different behavior was observed for the three types of particles. While the UV-Vis spectrum of AuNPs-**C1** was not affected by pH changes (**Figure 4A**), an aggregation was observed at pH2 in the case of AuNPs-**C3** but a further addition of NaOH redispersed cleanly the particles (**Figure 4C**). This reversible aggregation of AuNPs-**C3** was already described in the literature and is due to the protonation of the carboxylate groups of the grafted calixarenes under acidic conditions.[34] Interestingly, an intermediate behavior was observed for AuNPs-**C1/C3** upon pH variation (**Figure 4B**). Indeed, the difference between the λ_{max} at pH7 and pH2 ($\Delta\lambda_{max}$) for AuNPs-**C1/C3** is approximately half of that observed for AuNPs-**C3**. This gives a first indication that AuNPs-**C1/C3** are coated by a mixed layer of both calixarenes in similar proportions. The composition of the mixed layer of calixarenes was further analyzed by ATR-FTIR spectroscopy. A combination of the signals of AuNPs-**C1** (amide I and II and COC at 1664, 1542 and 1100 cm^{-1}, respectively) and AuNPs-**C3** (C=O at 1600 cm^{-1}) was observed for AuNPs-**C1/C3**, confirming the presence of the two calixarenes on the particles (**Figure 4D**). Furthermore, the intensities of the signals of amide I and COC were roughly half of the intensity of those of AuNPs-**C1** and AuNPs-**C3** respectively, suggesting a ca. 1:1 ratio of both calixarenes at the surface of AuNPs-**C1/C3 (Figure 4D, inset), as already observed for other combinations of calixarenes (see vide supra and refs 32 and 33)**. Finally, DLS analysis showed that the hydrodynamic radius of AuNPs-**C1**/**C3** was intermediate between those of AuNPs-**C1** and AuNPs-**C3** (Figure S9).

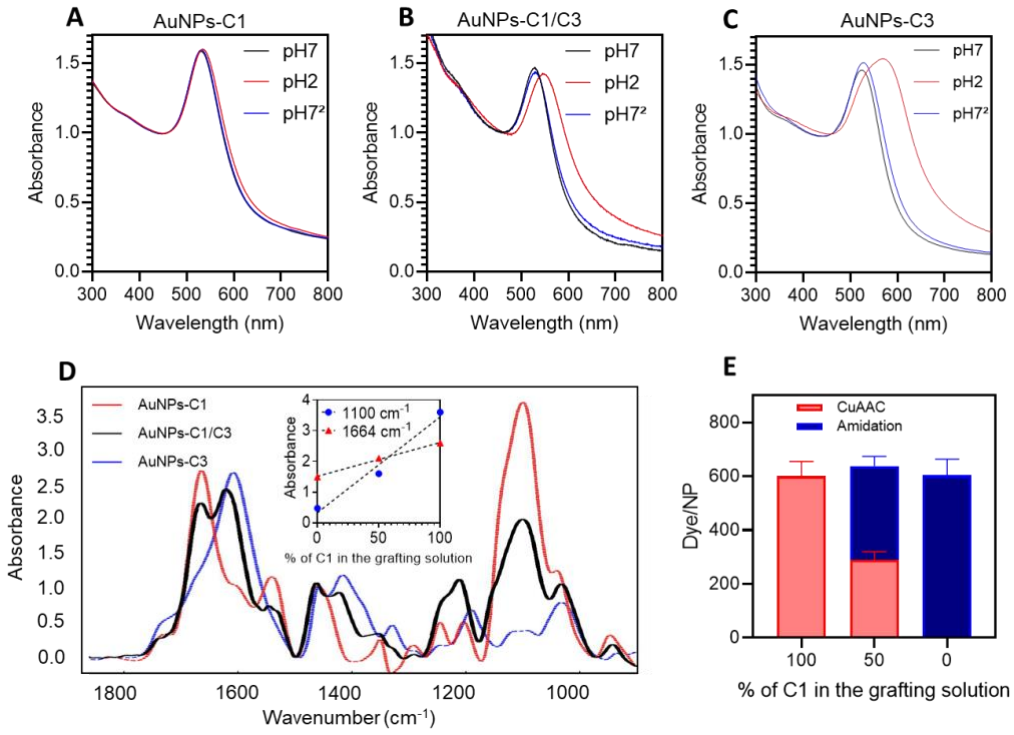

Figure 4. UV-Vis spectra of **(A)** AuNPs-**C1**, **(B)** AuNPs-**C1/C3** and **(C)** AuNPs-**C3** at pH7, pH2 and back to pH7. **(D)** FTIR spectra of AuNPs-**C1**, AuNPs-**C1/C3** and AuNPs-**C3**. Inset shows the absorbances at 1100 cm^{-1} (COC) and 1664 cm^{-1} (amide band I) as a function of the amount C1 used in the grafting solution. **(E)** Amount of N_3-cya7.5 or NH_2-cya7.5 dyes conjugated to the AuNPs-**C1**, AuNPs-**C1/C3** or AuNPs-**C3** either via CuAAC (red) or amidation (blue).

To demonstrate that AuNPs-**C1/C3** can be used as bifunctional AuNPs, the orthogonal conjugation of two dyes was evaluated via amide bond formation and CuAAC, respectively (**Scheme 2**). Two cyanine7.5-based dyes, i.e. H_2N-cya7.5 (see **Scheme 2** for the structure) and N_3-cya7.5, were used in order to avoid structural or physico-chemical differences (i.e. solubility, size, etc.) that could affect the conjugation and thus to have only the conjugation group that differs (i.e. amine or azide).

First, AuNPs-**C1/C3** were conjugated to H_2N-cya7.5 via a classical EDC/sulfo-NHS procedure and then cleaned from excess of reagents. The number of dyes covalently conjugated was measured by UV-Vis spectroscopy as described above (see Figure S10 for all the UV-Vis spectra). For comparison, experiments were also achieved with AuNPs-**C1** and AuNPs-**C3**

under the same conditions than for AuNPs-**C1**/**C3**. Estimations of 600±60 and 350±40 dyes conjugated per particles were found for AuNPs-**C3** and AuNPs-**C1**/**C3**, respectively, in agreement with the lower number of carboxyl groups at the surface of AuNPs-**C1**/**C3** (**Figure 4E**). In the case of AuNPs-**C1**, no UV-Vis absorption band around 800 nm was observed, as these particles carry no carboxyl groups for conjugation. Subsequent conjugation of N_3-cya7.5 was then performed via CuAAC on the different AuNPs that had been first reacted with NH_2-cya7.5. The number of dyes conjugated per particles was estimated to be 600 for AuNPs-**C1** while, as expected, no more dyes could be observed at the surface of AuNPs-**C3**. To our delight, a number of ca. 300±30 supplementary dyes was estimated at the surface of AuNPs-**C1**/**C3**. In other words, these particles were conjugated by a total of ca. 650 dyes (i.e. ca. 350 via amidation and ca. 300 via CuAAC), which roughly corresponds to the total of dyes carried by AuNPs-**C1** and AuNPs-**C3** (**Figure 4E**). Note that only tiny amount of dyes were detected on these different sets of particules when the conjugation experiments were conducted in the absence of coupling amidation or CuAAC reagents (Figure S11). These control experiments clearly show that the dyes are covalently linked onto the AuNPs and not only adsorbed.

Conclusion

Our bet was that calix[4]arene-tetradiazonium salts bearing alkynes and carboxyl groups could be used for the preparation of bifunctional gold nanoparticles that could be orthogonally post-functionalized. To do so, the synthesis of a new calixarene **C1** decorated with PEG chains ended by alkynes groups was first developed. The grafting of **C1** on AuNPs via a classical ligand-exchange procedure led to ultra-stable NPs that could be further post-functionalized through CuAAC. When mixtures of different ratios of **C1** and a similar calixarene deprived of alkyne groups (**C2**) were grafted, a control over the composition of the mixed layer was achieved. These first results are particularly attracting as the direct

functionalization of AuNPs with organic ligands bearing non protected terminal alkyne groups is far from trivial. The next step was to graft **C1** in association with a calix[4]arene-tetradiazonium salt bearing carboxyl groups (**C3**): AuNPs were coated with a mixed layer composed of approximately an equal amount of both calixarenes **C1** and **C3**. The subsequent conjugation of two dyes N_3-cya7.5 and NH_2-cya7.5 was performed through CuAAC and amide bond formation, respectively. Remarkably, a similar amount of each dye could be conjugated to these particles, as evidenced by UV-Vis spectroscopy. To our knowledge, this is the first example of bifunctional gold nanoparticles that can be simply conjugated with two different molecules in controlled ratios via different conjugation chemistries. Mixed layers of calixarenes bearing carboxyl and alkyne groups could be exploited for the orthogonal bioconjugation of nanomaterials with biomolecules such as peptides or DNA. Future work will be directed toward the use of this strategy for the design of new types of delivery systems based on multifunctional nanomaterials.

Experimental Section

Materials. Potassium gold (III) tetrachloride ($KAuCl_4$), trisodium citrate ($Na_3C_6H_5O_7$) were purchased from Sigma-Aldridge (Saint-Louis, MO). HS-$CH_2CH_2(CH_2CH_2O)_{12}$-$CH_2C{\equiv}CH$ (HS-PEG-alkyne, average Mn = 600 Da) was purchased from Nanocs Inc. (New-York, NY). All solutions were prepared with HPLC grade water (Lichrosolv®) and all reagent solutions were aqueous unless otherwise noted. Before use, all glassware and Teflon-coated stir bars were washed with aqua regia (3:1 volume ratio of concentrated HCl and HNO_3) and rinsed thoroughly with water. Caution: aqua regia is highly toxic and corrosive and requires proper personal protective equipment. Aqua regia should only be handled in a fume hood.

Gold nanoparticle synthesis. AuNPs were synthesized in an aqueous solution using a modified Turkevich method.[47] Briefly, in a three-neck round-bottom flask, 10 mL of trisodium

citrate (75 mM) were injected into 500 mL of boiling aqueous potassium gold (III) tetrachloride (0.3 mM) at pH 7. During the process, the reaction mixture changed quickly from yellow to orange then light red and finally bright red within one hour. The solution was refluxed for two hours and then quenched to room temperature. The freshly synthesized AuNPs suspension was then concentrated by decreasing the volume of the solution with a rotavapor. The final volume was between 100 mL and 150 mL and was then dialyzed against a 1 mM citrate solution during 6 h. This dialysis step was repeated three times, each with a fresh citrate solution. Images of the AuNPs were obtained with a Philips CM20-UltraTWIN Transmission Electron Microscope (TEM) equipped with a lanthanum hexaboride (LaB_6) crystal at a 200kV accelerating voltage. The average size and standard deviation were determined by measuring the size of more than 100 AuNPs and a core diameter of 19.7 ± 2.5 nm was measured. A concentration of 3.7 nM was determined by UV-Vis absorption spectroscopy, knowing the absorbance (A_{dil10x}= 0.35) and using the reported extinction coefficient by Liu *et al.* (2006) that is 9.5 $L.cm^{-1}.mol^{-1}$ for particles of that size.[48]

Calix[4]arene synthesis. C1 was synthesized in a few steps from commercial *pt*Bu-calix[4]arene-tetraacetic acid tetraethyl ester while **C2** and **C3** were readily obtained according to literature procedures.[28,33,35] Detailed synthesis and characterization of **C1** are presented in the Supporting Information.

Gold nanoparticles modification with calixarenes. Typically, 10 µL of $NaBH_4$ (0.1 M) were added to 0.8 mL of AuNPs-citrate (3.7 nM) under vigorous stirring in a glass vial containing a stir bar. Quickly after this, appropriate volume of calixarene aqueous solutions (5 mM) was added slowly (approximately 20 seconds for the complete addition) to reach 2×10^5 calixarenes/NP and the resulting suspensions were stirred over 16 hours at room temperature. The water dispersible nanoparticles were cleaned by centrifugation (20 minutes at 18.000g)

and replacement of the supernatant by an equivalent volume of milliQ water. This process was repeated four times.

Gold nanoparticles modification with HS-PEG-alkyne. 20 nm AuNPs-Citrate were functionalized with HS-$CH_2CH_2(CH_2CH_2O)_{12}$-$CH_2C{\equiv}CH$ (HS-PEG-alkyne) via a ligand-exchange method. Briefly, excess of HS-PEG-alkyne was added to AuNPs-citrate (>10^6 HS-PEG-alkyne/NP) under vigorous stirring at room temperature. After 16 hours of stirring, the functionalized gold nanoparticles (AuNPs-S-PEG-alkyne) were cleaned from the excess of HS-PEG-alkyne by four cycles of: (i) centrifugation (18000 g, 20 minutes), (ii) removal of the supernatant and (iii) dispersion of the NPs in pure water.

CuAAC conjugation of N_3-cya7.5. In a LoBind eppendorf, AuNPs were diluted in carbonate buffer (1 mM; pH 9) in order to reach a concentration of 0.4 nM in nanoparticles in a volume of 500 µL. 100 µL of DMSO were then added to ensure later the solubility of the dye. To this, 200 µL of sodium ascorbate (2 mM) were then added and the resulting mixture was degassed for 15 minutes. Finally, 200 µL of copper sulfate (2 mM) were added as well as an appropriate volume of N_3-cya7.5 to reach approximately 5000 dyes per particle. The temperature was then increased to 50 °C and the final mixture was stirred at 1000 rpm for four hours. It is worth to mention that initially the N_3-cya7.5 dye was dissolved in DMSO in order to make a highly concentrated mother solution (approximately 400 µM), the volume of dye added was thus neglectable compared to the total volume. At the end of the reaction, the AuNPs were cleaned from the excess of reagents and dyes by four cycles of centrifugation, removal of the supernatant and replacement of this latter by an aqueous SDS solution (1% in mass) to ensure the removal of non-conjugated dyes. SDS was used to resuspend the AuNPs for the three first centrifugation cycle and milliQ water was used for the final round.

Amide bond formation conjugation of H_2N-cya7.5 dye: In a LoBind eppendorf, AuNPs were diluted in phosphate buffer (50 mM, pH6.5) in order to reach a concentration of 0.4 nM in

nanoparticles in a volume of 250 µL. To this, 100 µL of DMSO were added to ensure later the solubility of the dye. Finally, 125 µL of an aqueous solution of EDC (6 mM) and 125 µL of an aqueous solution of sulfo-NHS (10 mM) were added, followed by the addition of the appropriate volume of H_2N-cya7.5 to reach approximately 5000 dyes per particle. The temperature was then increased to 50 °C and the final mixture was stirred at 1000 rpm for four hours. It is worth mentioning that the H_2N-cya7.5 dye was initially dissolved in DMSO in order to make a highly concentrated mother solution (approximately 400 µM), the volume of dye added was thus neglectable compared to the total volume. At the end of the reaction, the AuNPs were cleaned from the excess of reagents and dyes by four cycles of centrifugation, removal of the supernatant and replacement of this latter by an aqueous SDS solution (1% in mass) to ensure the removal of non-conjugated dyes. SDS was used to resuspend the AuNPs for the three first centrifugation cycle and milliQ water was used for the final round.

Conjugation quantification: After the cleaning step, UV-Vis spectroscopy was used to quantify the amount of N_3-cya7.5- or H_2N-cya7.5 dyes conjugated to the AuNPs.

The procedure was the following:

(i) The total absorbance at 805 nm was measured, corresponding to the absorbance of the dyes and the absorbance of the LSPR band of the particles.

(ii) The contribution of the LSPR band of the AuNPs at 805 nm was obtained with a polynomial fit between the regions 630-660 nm and 900-1000 nm.

(iii) The dye contribution at 805 nm was obtained by subtracting (ii) from (i) and the dye concentration was obtained thanks to its extinction coefficient (223.000 $L.mol^{-1}.cm^{-1}$).

(iv) The amount of dye adsorbed onto the particles and not covalently conjugated was obtained by performing steps (i), (ii) and (iii) in the absence of reagents (copper or EDC/NHS for CuAAC or amidation, respectively).

(v) The amount of dyes covalently conjugated to the AuNPs was obtained by subtracting (iv) from (iii) and by comparing this concentration to the AuNPs concentration determined by the absorbance at λ_{max} (assuming that the absorbance of the dye at 525 nm was neglectable).

ATR-FTIR analysis. ATR-FTIR spectra were recorded at 20°C on a Bruker Equinox 55 spectrophotometer equipped with a liquid nitrogen-cooled mercury−cadmium−telluride (MCT) detector. Typically, AuNPs were centrifuged (10 minutes, 20000g) and 1 µL of the AuNPs pellet was dried on a Germanium internal reflection crystal (triangular prism of 6.8 × 45 mm^2 with an internal angle of incidence of 45°, ACM France) with a flow of nitrogen gas. Opus software (4.2.37) was used to record 128 scans with a resolution of 2 cm^{-1} under a continuous flow of nitrogen gas over the sample. Data were processed and analyzed using the home-written Kinetics package in Matlab R2013a (Mathworks Inc., Natick, MA) by the subtraction of water vapor, baseline correction, apodization at 8 cm^{-1}, and flattening of the CO_2 signal. Finally, the spectra were normalized at 1456 cm^{-1} (C_{ar}-C_{ar} ring stretching band from the calix[4]arenes) to compensate for variations in the number of AuNPs present on the spot where the measurement was performed.

Supporting Information. Detailed procedures for the preparation of the synthesized compounds **C1**, **C2** and **C3**; NMR spectra of all the new compounds; characterization data of AuNPs-citrate, AuNPs-S-PEG-alkyne, AuNPs-S-PEG-cya7.5, AuNPs-C1/C2 and AuNPs-C1/C3; stability tests with AuNPS-C1; UV-vis spectrum of N_3-cya7.5 are available free of charge on the ACS Publications website at DOI: XXX.

Acknowledgements

The “Actions de Recherches Concertées” of the Fédération Wallonie-Bruxelles (Ph.D. grant to M. R., postdoc grant to B. C.) are acknowledged for financial support.

Conflict of Interest

M. R. was a postdoctoral researcher for X4C from August 2020 to January 2021. I. J. is a shareholder of X4C. I. J. and G.B. are consultants for X4C.

References

(1) Saha, K.; Agasti, S. S.; Kim, C.; Li, X.; Rotello, V. M. Gold Nanoparticles in Chemical and Biological Sensing. *Chem. Rev.* **2012**, *112* (5), 2739–2779. https://doi.org/10.1021/cr2001178.

(2) Zhou, W.; Gao, X.; Liu, D.; Chen, X. Gold Nanoparticles for in Vitro Diagnostics. *Chem. Rev.* **2015**, *115* (19), 10575–10636. https://doi.org/10.1021/acs.chemrev.5b00100.

(3) Elahi, N.; Kamali, M.; Baghersad, M. H. Recent Biomedical Applications of Gold Nanoparticles: A Review. *Talanta* **2018**, *184*, 537–556. https://doi.org/10.1016/j.talanta.2018.02.088.

(4) Nel, A. E.; Miller, J. F. Nano-Enabled COVID-19 Vaccines: Meeting the Challenges of Durable Antibody plus Cellular Immunity and Immune Escape. *ACS Nano* **2021**, *15* (4), 5793–5818. https://doi.org/10.1021/acsnano.1c01845.

(5) Kelly, K. L.; Coronado, E.; Zhao, L. L.; Schatz, G. C. The Optical Properties of Metal Nanoparticles: The Influence of Size, Shape, and Dielectric Environment. *J. Phys. Chem. B* **2003**, *107* (3), 668–677. https://doi.org/10.1021/jp026731y.

(6) Jain, P. K.; Huang, X.; El-Sayed, I. H.; El-Sayed, M. A. Review of Some Interesting Surface Plasmon Resonance-Enhanced Properties of Noble Metal Nanoparticles and Their Applications to Biosystems. *Plasmonics* **2007**, *2*, 107–118. https://doi.org/10.1007/s11468-007-9031-1.

(7) Maccora, D.; Dini, V.; Battocchio, C.; Fratoddi, I.; Cartoni, A.; Rotili, D.; Castagnola, M.; Faccini, R.; Bruno, I.; Scotognella, T.; Giordano, A.; Venditti, I. Gold Nanoparticles and Nanorods in Nuclear Medicine: A Mini Review. *Appl. Sci.* **2019**, *9* (16), 3232. https://doi.org/10.3390/app9163232.

(8) Kumar, A.; Ma, H.; Zhang, X.; Huang, K.; Jin, S.; Liu, J.; Wei, T.; Cao, W.; Zou, G.; Liang, X.-J. Gold Nanoparticles Functionalized with Therapeutic and Targeted Peptides for Cancer Treatment. *Biomaterials* **2012**, *33*, 1180–1189. https://doi.org/10.1016/j.biomaterials.2011.10.058.

(9) Majzik, A.; Fülöp, L.; Csapó, E.; Bogár, F.; Martinek, T.; Penke, B.; Bíró, G.; Dékány, I. Functionalization of Gold Nanoparticles with Amino Acid, Beta-Amyloid Peptides and Fragment. *Colloids and Surfaces B: Biointerfaces* **2010**, *81*, 235–241. https://doi.org/10.1016/j.colsurfb.2010.07.011.

(10) Zong, J.; Cobb, S. L.; Cameron, N. R. Peptide-Functionalized Gold Nanoparticles: Versatile Biomaterials for Diagnostic and Therapeutic Applications. *Biomater. Sci.* **2017**, *5*, 872–886. https://doi.org/10.1039/C7BM00006E.
(11) Jazayeri, M. H.; Amani, H.; Pourfatollah, A. A.; Pazoki-Toroudi, H.; Sedighimoghaddam, B. Various Methods of Gold Nanoparticles (GNPs) Conjugation to Antibodies. *Sens Biosensing Res* **2016**, *9*, 17–22. https://doi.org/10.1016/j.sbsr.2016.04.002.
(12) Zhang, C.; Wu, R.; Li, Y.; Zhang, Q.; Yang, J. Programmable Regulation of DNA Conjugation to Gold Nanoparticles via Strand Displacement. *Langmuir* **2017**, *33* (43), 12285–12290. https://doi.org/10.1021/acs.langmuir.7b02620.
(13) He, H.; Dai, J.; Duan, Z.; Zheng, B.; Meng, Y.; Guo, Y.; Xiao, D. Unusual Sequence Length-Dependent Gold Nanoparticles Aggregation of the SsDNA Sticky End and Its Application for Enzyme-Free and Signal Amplified Colorimetric DNA Detection. *Sci. Rep.* **2016**, *6* (24), 1–7. https://doi.org/10.1038/srep30878.
(14) Lesniewski, A.; Los, M.; Jonsson-Niedzioὶåka, M.; Krajewska, A.; Szot, K.; Los, J. M.; Niedziolka-Jonsson, J. Antibody Modified Gold Nanoparticles for Fast and Selective, Colorimetric T7 Bacteriophage Detection. *Bioconjugate Chem.* **2014**, *25* (4), 644–648. https://doi.org/10.1021/bc500035y.
(15) Mohd-Zahid, M. H.; Mohamud, R.; Che Abdullah, C. A.; Lim, J.; Alem, H.; Wan Hanaffi, W. N.; Iskandar, Z. A. Colorectal Cancer Stem Cells: A Review of Targeted Drug Delivery by Gold Nanoparticles. *RSC Adv.* **2019**, *10* (2), 973–985. https://doi.org/10.1039/c9ra08192e.
(16) Kong, F. Y.; Zhang, J. W.; Li, R. F.; Wang, Z. X.; Wang, W. J.; Wang, W. Unique Roles of Gold Nanoparticles in Drug Delivery, Targeting and Imaging Applications. *Molecules* **2017**, *22* (9), 1445. https://doi.org/10.3390/molecules22091445.
(17) Yao, C.; Zhang, L.; Wang, J.; He, Y.; Xin, J.; Wang, S.; Xu, H.; Zhang, Z. Gold Nanoparticle Mediated Phototherapy for Cancer. *Journal of Nanomaterials* **2016**, *2016*, 5497136. https://doi.org/10.1155/2016/5497136.
(18) Amendoeira, A.; García, L. R.; Fernandes, A. R.; Baptista, P. v. Light Irradiation of Gold Nanoparticles Toward Advanced Cancer Therapeutics. *Adv. Therap.* **2020**, *3* (1), 1900153. https://doi.org/10.1002/adtp.201900153.
(19) Smith, A. M.; Marbella, L. E.; Johnston, K. A.; Hartmann, M. J.; Crawford, S. E.; Kozycz, L. M.; Seferos, D. S.; Millstone, J. E. Quantitative Analysis of Thiolated Ligand Exchange on Gold Nanoparticles Monitored by 1H NMR Spectroscopy. *Anal. Chem.* **2015**, *87* (5), 2771–2778. https://doi.org/10.1021/ac504081k.
(20) Retout, M.; Brunetti, E.; Valkenier, H.; Bruylants, G. Limits of Thiol Chemistry Revealed by Quantitative Analysis of Mixed Layers of Thiolated-PEG Ligands Grafted onto Gold Nanoparticles. *Journal of Colloid and Interface Science* **2019**, *557*, 807–815. https://doi.org/10.1016/j.jcis.2019.09.047.
(21) Mullen, D. G.; Banaszak Holl, M. M. Heterogeneous Ligand-Nanoparticle Distributions: A Major Obstacle to Scientific Understanding and Commercial Translation. *Acc. Chem. Res.* **2011**, *44* (11), 1135–1145. https://doi.org/10.1021/ar1001389.
(22) Zeiri, O. Metallic-Nanoparticle-Based Sensing: Utilization of Mixed-Ligand Monolayers. *ACS Sens.* **2020**, *5* (12), 3806–3820. https://doi.org/10.1021/acssensors.0c02124.
(23) Tkachenko, A. G.; Xie, H.; Coleman, D.; Glomm, W.; Ryan, J.; Anderson, M. F.; Franzen, S.; Feldheim, D. L. Multifunctional Gold Nanoparticle-Peptide Complexes for Nuclear

Targeting. *J. Am. Chem. Soc.* **2003**, *125* (16), 4700–4701. https://doi.org/10.1021/ja0296935.
(24) Conde, J.; Ambrosone, A.; Sanz, V.; Hernandez, Y.; Marchesano, V.; Tian, F.; Child, H.; Berry, C. C.; Ibarra, M. R.; Baptista, P. v.; Tortiglione, C.; de La Fuente, J. M. Design of Multifunctional Gold Nanoparticles for in Vitro and in Vivo Gene Silencing. *ACS Nano* **2012**, *6* (9), 8316–8324. https://doi.org/10.1021/nn3030223.
(25) Mieszawska, A. J.; Mulder, W. J. M.; Fayad, Z. A.; Cormode, D. P. Multifunctional Gold Nanoparticles for Diagnosis and Therapy of Disease. *Mol. Pharmaceutics* **2013**, *10* (3), 831–847. https://doi.org/10.1021/mp3005885.
(26) Wang, Z.; Lévy, R.; Fernig, D. G.; Brust, M. The Peptide Route to Multifunctional Gold Nanoparticles. *Bioconjugate Chem.* **2005**, *16* (3), 497–500. https://doi.org/10.1021/bc050047f.
(27) Liu, T.; Thierry, B. A Solution to the PEG Dilemma: Efficient Bioconjugation of Large Gold Nanoparticles for Biodiagnostic Applications Using Mixed Layers. *Langmuir* **2012**, *28* (44), 15634–15642. https://doi.org/10.1021/la301390u.
(28) Pinson, J.; Podvoricab, F. Attachment of Organic Layers to Conductive or Semiconductive Surfaces by Reduction of Diazonium Salts. *Chem. Soc. Rev.* **2005**, *34*, 429–439.
(29) Yates, N. D.; Dowsett, M. R.; Bentley, P.; Dickenson-Fogg, J. A.; Pratt, A.; Blanford, C. F.; Fascione, M. A.; Parkin, A. Aldehyde-Mediated Protein-to-Surface Tethering via Controlled Diazonium Electrode Functionalization Using Protected Hydroxylamines. *Langmuir* **2020**, *36* (20), 5654–5664. https://doi.org/10.1021/acs.langmuir.9b01254.
(30) Jiang, C.; Moraes Silva, S.; Fan, S.; Wu, Y.; Alam, M. T.; Liu, G.; Justin Gooding, J. Aryldiazonium Salt Derived Mixed Organic Layers: From Surface Chemistry to Their Applications. *Journal of Electroanalytical Chemistry* **2017**, *785*, 265–278. https://doi.org/10.1016/j.jelechem.2016.11.043.
(31) Ludovic Troian-Gautier, Alice Mattiuzzi, Olivia Reinaud, C. L. and I. J. Use of Calixarenes Bearing Diazonium Groups for the Development of Robust Monolayers with Unique Tailored Properties. *Org. Biomol. Chem.* **2020**, *18*, 3624–3637.
(32) Mattiuzzi, A.; Jabin, I.; Mangeney, C.; Roux, C.; Reinaud, O.; Santos, L.; Bergamini, J. F.; Hapiot, P.; Lagrost, C. Electrografting of Calix[4]Arenediazonium Salts to Form Versatile Robust Platforms for Spatially Controlled Surface Functionalization. *Nat Commun* **2012**, *3*, 1130. https://doi.org/10.1038/ncomms2121.
(33) Li, H.; Kopiec, G.; Müller, F.; Nyßen, F.; Shimizu, K.; Ceccato, M.; Daasbjerg, K.; Plumeré, N. Spectroscopic Evidence for a Covalent Sigma Au–C Bond on Au Surfaces Using 13 C Isotope Labeling . *JACS Au* **2021**, *1* (3), 362–368. https://doi.org/10.1021/jacsau.0c00108.
(34) Ludovic Troian-Gautier; Valkenier, H.; Mattiuzzi, A.; Jabin, I.; van den Brande, N.; van Mele, B.; Hubert, J.; Reniers, F.; Bruylants, G.; Lagrost, C.; Leroux, Y. Extremely Robust and Post-Functionalizable Gold Nanoparticles Coated with Calix[4]Arenes via Metal–Carbon Bonds. *Chem. Commun.* **2016**, *52*, 10493–10496. https://doi.org/10.1039/c6cc04534k.
(35) Retout, M.; Jabin, I.; Bruylants, G. Synthesis of Ultrastable and Bioconjugable Ag, Au, and Bimetallic Ag_Au Nanoparticles Coated with Calix[4]Arenes. *ACS Omega* **2021**, *6*, 19675–19684. https://doi.org/https://doi.org/10.1021/acsomega.1c02327.
(36) Ahmad, A. A. L.; Marutheri Parambath, J. B.; Postnikov, P. S.; Guselnikova, O.; Chehimi, M. M.; Bruce, M. R. M.; Bruce, A. E.; Mohamed, A. A. Conceptual

Developments of Aryldiazonium Salts as Modifiers for Gold Colloids and Surfaces. *Langmuir* **2021**, *37* (30), 8897–8907. https://doi.org/10.1021/acs.langmuir.1c00884.
(37) Blond, P.; Bevernaegie, R.; Troian-Gautier, L.; Lagrost, C.; Hubert, J.; Reniers, F.; Raussens, V.; Jabin, I. Ready-to-Use Germanium Surfaces for the Development of FTIR-Based Biosensors for Proteins. *Langmuir* **2020**, *36*, 12068–12076. https://doi.org/10.1021/acs.langmuir.0c02681.
(38) Retout, M.; Blond, P.; Jabin, I.; Bruylants, G. Ultrastable PEGylated Calixarene-Coated Gold Nanoparticles with a Tunable Bioconjugation Density for Biosensing Applications. *Bioconjugate Chem.* **2021**, *32*, 290–300. https://doi.org/10.1021/acs.bioconjchem.0c00669.
(39) Valkenier, H.; Malytskyi, V.; Blond, P.; Retout, M.; Mattiuzzi, A.; Goole, J.; Raussens, V.; Jabin, I.; Bruylants, G. Controlled Functionalization of Gold Nanoparticles with Mixtures of Calix[4]Arenes Revealed by Infrared Spectroscopy. *Langmuir* **2017**, *33*, 8253–8259. https://doi.org/10.1021/acs.langmuir.7b02140.
(40) Santos, L.; Mattiuzzi, A.; Jabin, I.; Vandencasteele, N.; Reniers, F.; Reinaud, O.; Hapiot, P.; Lhenry, S.; Leroux, Y.; Lagrost, C. One-Pot Electrografting of Mixed Monolayers with Controlled Composition. *J. Phys. Chem. C* **2014**, *118* (29), 15919–15928. https://doi.org/10.1021/jp5052003.
(41) Kendziora, D. M.; Ahmed, I.; Fruk, L. Multifunctional Linker for Orthogonal Decoration of Gold Nanoparticles with DNA and Protein. *RSC Adv.* **2014**, *4* (35), 17980–17985. https://doi.org/10.1039/c4ra01773k.
(42) Lenne, Q.; Retout, M.; Gosselin, B.; Bruylants, G.; Jabin, I.; Hamon, J.; Lagrost, C.; Leroux, Y. R. Highly Stable Silver Nanohybrid Electrocatalysts for the Oxygen Reduction Reaction. *Chem. Commun.* **2022**, *58*, 3334–3337.
(43) Poonthiyil, V.; Lindhorst, T. K.; Golovko, V. B.; Fairbanks, A. J. Recent Applications of Click Chemistry for the Functionalization of Gold Nanoparticles and Their Conversion to Glyco-Gold Nanoparticles. *Beilstein J. Org. Chem.* **2017**, *14*, 11–24. https://doi.org/10.3762/bjoc.14.2.
(44) Maity, P.; Takano, S.; Yamazoe, S.; Wakabayashi, T.; Tsukuda, T. Binding Motif of Terminal Alkynes on Gold Clusters. *J. Am. Chem. Soc.* **2013**, *135*, 9450–9457. https://doi.org/10.1021/ja401798z.
(45) Fracasso, D.; Kumar, S.; Chiechi, R. C. Self-Assembled Monolayers of Terminal Acetylenes as Replacements for Thiols in Bottom-up Tunneling Junctions. *RSC Adv.* **2014**, *4*, 56026–56030. https://doi.org/10.1039/C4RA09880C.
(46) Zhou, Y.; Wang, S.; Zhang, K.; Jiang, X. Visual Detection of Copper(II) by Azide- and Alkyne-Functionalized Gold Nanoparticles Using Click Chemistry. *Angew Chem Int Ed Engl.* **2008**, *47* (39), 7454–7456. https://doi.org/10.1002/anie.200802317.
(47) Doyen, M.; Bartik, K.; Bruylants, G. UV-Vis and NMR Study of the Formation of Gold Nanoparticles by Citrate Reduction: Observation of Gold-Citrate Aggregates. *Journal of Colloid and Interface Science* **2013**, *399*, 1–5. https://doi.org/10.1016/j.jcis.2013.02.040.
(48) Liu, X.; Atwater, M.; Wang, J.; Huo, Q. Extinction Coefficient of Gold Nanoparticles with Different Sizes and Different Capping Ligands. *Colloids Surf B Biointerfaces* **2007**, *58* (1), 3–7. https://doi.org/10.1016/j.colsurfb.2006.08.005.